RESEARCH PAPER

LC-HRMS-Based Phytochemical Profiling and Computational Evaluation of Butea monosperma Against IGF2R

Galla Likitha[1], P. Dharani Prasad[1]*

.

[1]*Department of Pharmacology, School of Pharmaceutical Sciences (Erstwhile Sree Vidyaniketan College of Pharmacy), Mohan Babu University, Tirupati 517102, Andhra Pradesh, India*

Received: 21st Aug, 2025; Revised: 02nd Sep 2025; Accepted: 17th Nov, 2025; Available Online: 30th Nov, 2025

ABSTRACT

The present study aimed to comprehensively evaluate the phytochemical composition and therapeutic potential of *Butea monosperma* through experimental and computational approaches. Hydroalcoholic extraction yielded a stable, dark brownish extract with a 10.5% yield, near-neutral pH, low moisture content, and acceptable ash values, confirming purity and stability. Microbial evaluation demonstrated absence of pathogenic organisms, validating its safety for therapeutic applications. Preliminary phytochemical screening revealed abundant flavonoids and phenolics, along with moderate levels of tannins, glycosides, anthraquinones, and saponins, supporting its pharmacological relevance. LC-HRMS profiling identified five major bioactive constituents—quercetin, rutin, kaempferol-3-O-rutinoside, apigenin-7-O-glucoside, and soyasaponin I—compounds well-known for antioxidant, anti-inflammatory, cardioprotective, and anticancer properties. Molecular docking studies targeting Insulin-like Growth Factor Receptor Type-2 (IGF2R) revealed rutin (−9.3 kcal/mol) and quercetin (−8.2 kcal/mol) exhibited superior binding affinities compared to the NL-2V5O (Native Ligand) (−6.6 kcal/mol), forming stable hydrogen bonding, hydrophobic, and electrostatic interactions. Apigenin-7-O-glucoside and kaempferol-3-O-rutinoside showed moderate binding, while soyasaponin I displayed binding comparable to the NL-2V5O. ADMET predictions provided insight into pharmacokinetic and toxicity profiles. Quercetin demonstrated the most balanced drug-likeness, with favorable absorption and bioavailability, though limited by high plasma protein binding and metabolic interactions. Rutin and kaempferol-3-O-rutinoside showed restricted intestinal absorption, whereas soyasaponin I exhibited strong bioavailability but raised toxicity concerns. Apigenin-7-O-glucoside showed moderate promise with minimal rule violations. In conclusion, *B. monosperma* is a flavonoid-rich medicinal plant with significant therapeutic potential. Quercetin emerged as the most promising lead compound, warranting further in vivo validation and formulation strategies to enhance its bioavailability and clinical applicability...

Keywords: Butea monosperma, LC-HRMS, Molecular docking, ADMET analysis, IGF2R, Phytochemical profiling.

How to cite this article: Likitha G, Prasad PD. LC-HRMS-based phytochemical profiling and computational evaluation of *Butea monosperma* against IGF2R. Int J Drug Deliv Technol. 2025;15(4):1452-1467. DOI: 10.25258/ijddt.15.4.2

Source of support: Nil.

Conflict of interest: None

INTRODUCTION

Herbal medicine has been increasingly recognized worldwide as a promising alternative and complementary approach to conventional therapeutics. Plants are natural reservoirs of structurally diverse bioactive compounds, many of which exhibit significant pharmacological properties such as antioxidant, anti-inflammatory, anticancer, antimicrobial, and immunomodulatory effects. Secondary metabolites including flavonoids, alkaloids, terpenoids, glycosides, tannins, and phenolics have been studied extensively for their ability to modulate key biological pathways relevant to chronic diseases like diabetes, cardiovascular disorders, neurodegenerative conditions, and cancer. With the rising global burden of lifestyle-related disorders and the limitations of synthetic drugs, there has been a resurgence of interest in natural products as valuable scaffolds for drug discovery and therapeutic development[1,2,3,4,5].

Butea monosperma (family Fabaceae), commonly known as “Flame of the Forest” or “Palash,” is a well-known medicinal plant with cultural, ornamental, and therapeutic importance in the Indian subcontinent. It has been widely utilized in Ayurveda, Unani, and folk medicine for centuries. Different parts of the plant—including flowers, bark, seeds, and leaves—are traditionally used in the treatment of various ailments such as inflammation, ulcers, diabetes, liver disorders, infections, and reproductive health problems[6,7,8,9]. These ethnomedicinal applications provide a strong rationale for exploring its bioactive potential using modern scientific tools and approaches.

Advancements in analytical platforms have opened new avenues for understanding the complex chemical composition of medicinal plants. Techniques such as liquid chromatography coupled with high-resolution mass spectrometry (LC-HRMS) enable comprehensive profiling of phytochemicals with high accuracy and sensitivity. LC-HRMS allows for the tentative identification of metabolites based on mass, retention times, and fragmentation patterns, providing an in-depth chemical fingerprint of herbal extracts. Such methods not only validate the knowledge

**Author for Correspondence: dharaniprasadp@gmail.com*

derived from traditional medicine but also uncover novel bioactive compounds that may serve as leads in drug discovery[10,11,12]. In the case of *B. monosperma*, the application of LC-HRMS offers the opportunity to establish a detailed phytochemical profile, ensuring scientific validation of its medicinal relevance.

GRAPHICAL ABSTRACT

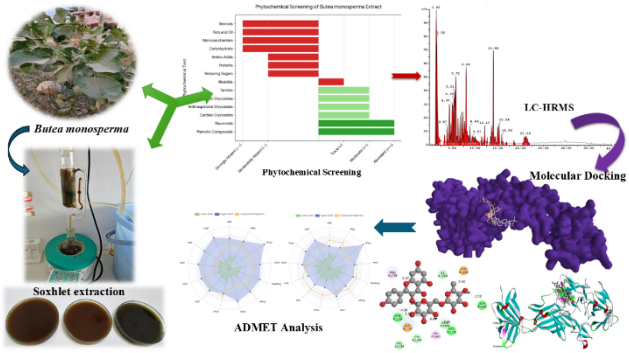

Parallel to analytical studies, computational approaches have become indispensable in pharmacognosy and modern drug discovery. Molecular docking provides insights into how specific phytochemicals interact with disease-related protein targets, predicting binding affinities and interaction mechanisms. This approach allows researchers to identify compounds with potential therapeutic effects even before conducting in-depth biological studies. Complementing docking studies, ADMET (Absorption, Distribution, Metabolism, Excretion, and Toxicity) analysis is employed to predict the pharmacokinetics and safety profiles of candidate molecules [13,14,15,16]. Together, these computational tools provide a holistic understanding of the pharmacological potential of plant-derived compounds, allowing for the prioritization of promising leads for further development.

One molecular target of growing interest in cancer and metabolic disease research is the Insulin-like Growth Factor Receptor Type-2 (IGF2R). This receptor plays a key role in regulating cellular processes such as growth, apoptosis, and signaling pathways linked to tumor progression. Dysregulation of IGF2R has been implicated in cancer biology, making it a valuable therapeutic target. Natural compounds that can interact with and modulate the activity of IGF2R may hold significant promise in oncology and other disease contexts[17,18,19,20]. Considering the traditional uses of *B. monosperma* and the therapeutic relevance of its phytochemical classes, a detailed evaluation of its interaction with IGF2R is both timely and necessary.

Integrating advanced analytical techniques with computational studies creates a robust framework for the exploration of medicinal plants. For *B. monosperma*, such an approach allows for the identification and evaluation of key phytoconstituents, the prediction of their binding affinities with clinically relevant targets, and the assessment of their pharmacokinetic and safety characteristics. This not only strengthens the scientific foundation underlying its traditional use but also provides a rational basis for its potential application in modern therapeutics. Ultimately, exploring the phytochemical and pharmacological aspects of *B. monosperma* through LC-HRMS profiling, molecular docking, and ADMET predictions can contribute significantly to the discovery of novel bioactive compounds with clinical relevance, thereby bridging the gap between traditional medicine and modern drug development.

MATERIALS AND METHOD

Drugs, Chemicals, Reagents, Apparatus, and Instruments

The present research work utilized a wide range of chemicals and reagents, including crystal iodine, hydrochloric acid, ethyl acetoacetate (Molychem, Mumbai, India), 0.9% sodium chloride (Avra Chemicals), and precoated aluminum silica gel plates (E. Merck, Germany), along with other solvents, acids, bases, and analytical reagents essential for experimental procedures. Apparatus employed comprised Soxhlet's extractor (Lab Trading Laboratory, Aurangabad), separating funnel, round bottom flask, reflux assembly, TLC plates, and rotary evaporator (Buchi, Switzerland), while instruments such as heating mantle (TOPLAB India), magnetic stirrer (Remi), and digital melting point apparatus (SESW) were used to ensure precise extraction, analysis, and characterization throughout the study.

Collection of Plant Material and Authentication

B. monosperma herb was collected in December 2024 from the local area of Nalgonda, Telangana, India. From the collected plant material, the herbarium was prepared and authenticated by Dr. K. Madhava Chetty, Head of Botanical Department of Sri Venkateswara University, Tirupati, 517502, Andhra Pradesh, India. A voucher specimen no. 0329 was deposited. After collecting authentication certificate, the extraction procedure was performed. The images of the plant are depicted in Figure 1.

Figure 1. The *B. monosperma* plant collected from XYZ District

Soxhlet Extraction using Hydroalcoholic Solvent

For extraction, *B. monosperma's* leaves and bark were collected and washed them using distilled water to remove any dust or foreign particle, and then air-dried in the shade for a week at room temperature. It is essential to dry it in room temperature to avoid the loss of volatile phytoconstituents. About 500 grams of dried plant material was grinded into a course powder for further extraction process. The resulting powder was subjected for Soxhlet extraction using Soxhlet apparatus by hydroalcoholic solvent (Ethanol:water; 70:30). The extraction process was continued until complete isolation of secondary metabolites present in plant material. The dark green color of the solvent in RBF and fainted color of plant material in Soxhlet extractor denoted the successive isolation of constituents. At least 24 hours were devoted for the extraction and during this meantime several siphon cycles were completed. The contents of the RFB then poured into different petri plates and the solvent was allowed to evaporate naturally for few hours. The concentrated extract was then subjected for different qualitative analysis tests[21,22,23]. The working photographs of Soxhlet extraction are depicted in Figure 2 .

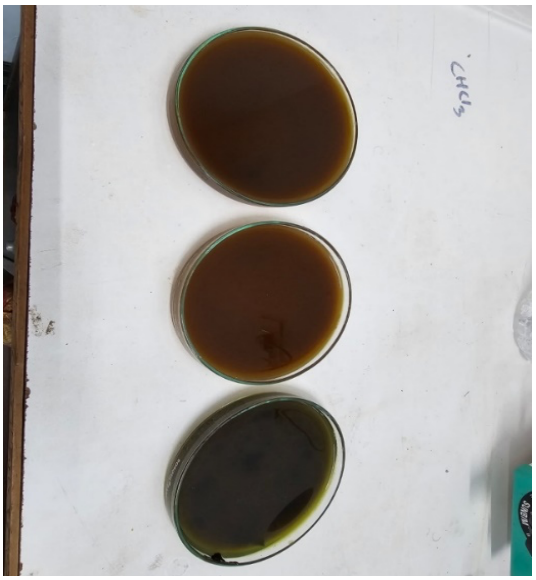

Figure 2. The Soxhlet extraction of *B. monosperma*

Physicochemical Analysis

The physicochemical evaluation of the extracts was carried out following standard procedures. Organoleptic properties including colour were assessed under natural light, while odour and taste were examined directly by olfactory and gustatory perception. pH determination was performed for 1% and 10% aqueous solutions of extracts using a digital pH meter for accuracy. Foreign matter was separated, weighed, and expressed as percentage contamination. Moisture content was determined by loss on drying (LOD) at 105 °C until constant weight was achieved. Ash values including total ash, acid-insoluble ash, sulphated ash, and water-soluble ash were measured by incineration, chemical treatment, and gravimetric analysis. Extractive values were determined by macerating powdered drug in alcohol and chloroform water, followed by filtration, drying, and calculation of percentage yield[24,25]. Heavy metal estimation was performed using microwave digestion with HNO3, followed by atomic absorption spectrometry under standard operating conditions to quantify arsenic, cadmium, lead, mercury, zinc, copper, chromium, and manganese. Pesticide residue analysis was conducted by concentrating extracts with a rotary evaporator, passing them through a clean-up column, and analyzing aliquots using GC with an electron capture detector under controlled temperature and nitrogen flow, ensuring sensitivity in the range of 0.1–0.5 ppb [26,27].

Phytochemical and Microbial Evaluation

Preliminary phytochemical profiling of the crude extract was performed using standard qualitative assays, confirming the presence of key metabolites including carbohydrates, proteins, amino acids, lipids, steroids, glycosides, flavonoids, alkaloids, tannins, and phenolics through colorimetric and precipitation reactions. Saponins, anthraquinones, and cyanogenetic glycosides were also detected by characteristic foam, Borntrager's, and picrate-based tests, respectively. Microbial evaluation involved serial dilutions of samples and cultivation on selective agar media to estimate total bacterial and fungal load, while specific pathogens were screened using enrichment and differential media: E. coli (MacConkey broth), Salmonella

spp. (Selenite/Tetrathionate broth with DCA), Shigella spp. (SS agar with biochemical confirmation), Pseudomonas aeruginosa (cetrimide agar with oxidase test), and Staphylococcus aureus (MSA with catalase and coagulase tests). All procedures were standardized to ensure reproducibility and accuracy[24,25,28,29,30].

LC-HRMS Analysis

LC-HRMS profiling of the extract was performed using an ACCUCORE C18 column (150 × 4.6 mm, 2.6 µm) under reversed-phase conditions. The dried sample was dissolved in HPLC-grade methanol, filtered (0.22 µm), and injected for analysis. Chromatographic separation was carried out with a binary mobile phase of water and acetonitrile (both containing 0.1% formic acid) under a gradient program at a flow rate of 0.3–0.5 mL/min. Mass detection was achieved in both positive and negative electrospray ionization (ESI) modes across an m/z range of 50–1500, with high-resolution full scans followed by data-dependent MS/MS fragmentation for structural elucidation. Instrument parameters such as capillary voltage, nebulizer gas, and desolvation conditions were optimized to ensure high ionization efficiency. The acquired data were processed using vendor software, and tentative compound identification was performed by matching accurate masses, retention times, and fragmentation patterns with public databases and literature [31,32,33].

Molecular Docking Analysis

Ligand Preparation

The bioactive constituents of *B. monosperma* identified through LC-HRMS analysis were selected for molecular docking studies. Ligand structures were initially draw using ChemDraw. For compounds with known structures, canonical SMILES or SDF files were retrieved from PubChem. All ligand molecules were subjected to energy minimization using the force field to obtain stable conformations. The final minimized structures were saved in mol format and later converted to pdbqt format using Open Babel within PyRx for docking purposes[13,14,15,16].

Protein Preparation

The crystal structure of Insulin-like Growth Factor Receptor Type-2 (IGF2R) was obtained from the RCSB Protein Data Bank (PDB ID: 2V5O). The protein structure was prepared using Discovery Studio, where water molecules, ligands, and heteroatoms were removed. Polar hydrogens were added, and the missing residues were corrected if necessary. The clean protein structure was saved in pdb format and imported into PyRx, where it was converted to pdbqt format using AutoDock Tools[13,14,15,16].

Molecular Docking

Molecular docking was performed using AutoDock Vina integrated within the PyRx 0.8 platform. The docking grid box was centered on the predicted active site of IGF2R, with the following coordinates: Center (XYZ): 77.632929, 16.356857, 10.174929. The grid box dimensions were optimized to encompass the binding pocket fully, ensuring the ligands had sufficient space for flexible conformational search. All docking parameters were kept at default values unless otherwise specified. The docking results were ranked based on binding affinity (kcal/mol), and the best pose for each ligand was selected for further interaction analysis. The docked complexes were visualized and analyzed using Discovery Studio Visualizer, focusing on hydrogen bonds, hydrophobic interactions, and key binding residues[13,14,15,16].3D representation of IGF2R enzyme with all selected derivatives and NL-2V5O are shown in Figure 3.

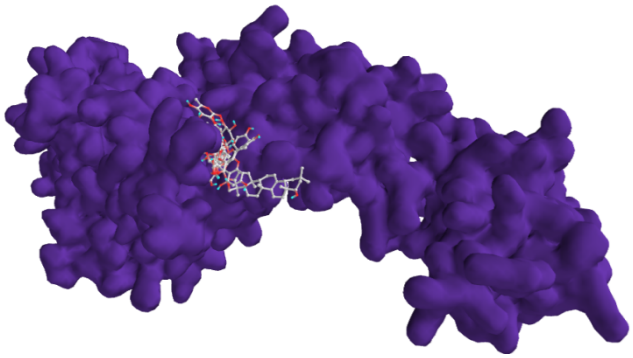

Figure 3. 3D representation of IGF2R enzyme (PDB ID: 2V5O) with all selected derivatives

ADMET analysis

The pharmacokinetic and toxicity profiles of the docked ligands were evaluated through in silico ADMET analysis to assess their drug-likeness and safety. The 2D structures of the selected compounds were initially drawn using ChemDraw, and the corresponding SMILES notations were generated. Alternatively, for known compounds, SMILES data were directly obtained from PubChem. The SMILES of each ligand were submitted to SwissADME (http://www.swissadme.ch/) to predict physicochemical properties, lipophilicity (LogP), solubility, pharmacokinetics, drug-likeness, and bioavailability scores. For a more detailed toxicity and metabolism profile, the same SMILES were analyzed using ADMETlab 3.0 (https://admetlab3.scbdd.com/server/evaluation), which provided data on absorption (e.g., Caco-2 permeability, P-glycoprotein interactions), distribution (e.g., volume of distribution, plasma protein binding), metabolism (CYP450 enzyme interactions), excretion (half-life and clearance), and toxicity parameters (such as hepatotoxicity, AMES mutagenicity, and hERG inhibition). All results were compiled and evaluated to identify potential lead compounds with favorable pharmacokinetic and toxicity profiles[13,14,15,16].

RESULTS AND DISCUSSIONS

Organoleptic and Physicochemical Analysis of Extracts

Hydroalcoholic extraction of *B. monosperma* yielded 10.5% of a solid dark brownish extract with an agreeable, slightly aromatic odour and bitter taste, features indicative of phenolic and glycosidic constituents. Physicochemical analysis of *B. monosperma* extract is shown in Figure 4. The extract exhibited near-neutral pH (6.8 in 1% and 6.3 in 10% solution), supporting its suitability for oral and topical use. Physicochemical evaluation showed acceptable ash values (total ash 7.81%, acid-insoluble ash 1.22%, water-soluble ash 2.97%, sulphated ash 1.32%), confirming minimal contamination and good purity. The loss on drying (4.67%) indicated low moisture content and stability, while extractive values revealed higher alcohol-soluble content

(17.97%) compared to water-soluble (14.56%), reflecting efficient recovery of semi-polar bioactives such as flavonoids and triterpenoids. Importantly, no heavy metals or pesticide residues were detected, validating the extract's safety profile. Overall, the organoleptic and physicochemical characteristics suggest that the hydroalcoholic extract of *B. monosperma* is pure, stable, and enriched with pharmacologically relevant phytoconstituents.

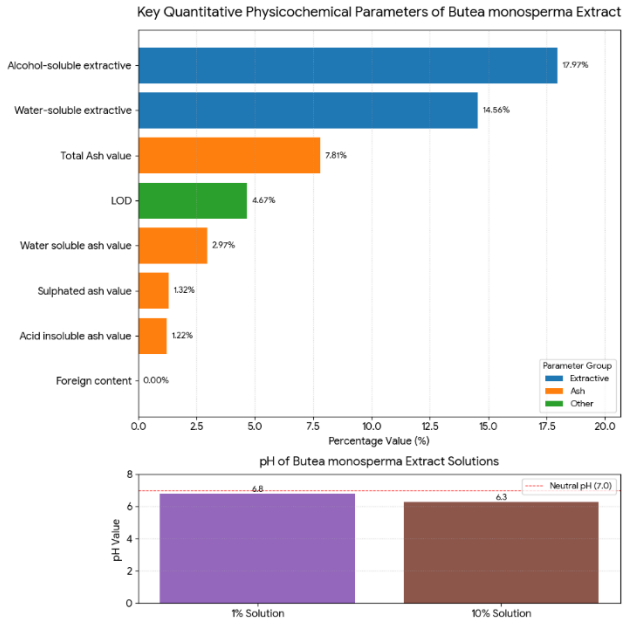

Figure 4. The physicochemical analysis of *B. monosperma* extract

Microbial and Phytochemical Evaluation of *B. monosperma* Extract

Microbiological testing confirmed that the hydro-alcoholic extract of *B. monosperma* was free from pathogenic microorganisms, including Escherichia coli, Salmonella spp., Shigella spp., Pseudomonas aeruginosa, and Staphylococcus aureus, thereby ensuring its microbial safety and reflecting proper hygienic handling during raw material processing and extraction. This safety aspect is particularly significant for herbal formulations intended for therapeutic use, especially in immunocompromised patients.

Preliminary phytochemical screening revealed the presence of several key bioactive constituents, with abundant levels of phenolic compounds and flavonoids (+++), moderate levels of tannins, cardiac glycosides, anthraquinone glycosides, and saponins (++), and trace levels of alkaloids (+) (Figure 5). These secondary metabolites are widely recognized for their diverse pharmacological properties such as antioxidant, anti-inflammatory, cardiotonic, antimicrobial, immunomodulatory, and neuroprotective activities. The high phenolic and flavonoid content aligns with literature reports linking *B. monosperma* to strong antioxidant and free radical scavenging effects, while the glycosidic compounds suggest additional therapeutic roles in cardiovascular regulation and metabolic modulation. Conversely, the extract tested negative for primary metabolites including carbohydrates, proteins, amino acids, fats, and steroids, indicating the selectivity of the hydro-alcoholic solvent system in extracting predominantly secondary metabolites.

Overall, the extract demonstrated excellent microbial quality and a rich phytochemical profile dominated by polyphenols and glycosides, thereby validating its therapeutic potential. These findings provide strong justification for its application in the development of antioxidant, cardioprotective, and anti-inflammatory herbal formulations.

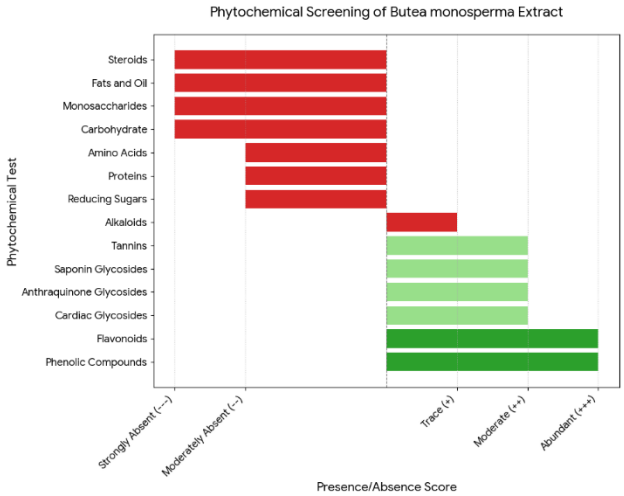

Figure 5. The results of preliminary phytochemical screening of *B. monosperma* extract

LC-HRMS analysis

The LC-HRMS analysis of the extract revealed multiple chromatographic peaks, with tentative identification of compounds based on accurate mass values, retention times, and fragmentation patterns (Table 1 and Figure 6). Five major constituents were identified: quercetin, rutin, kaempferol-3-O-rutinoside, apigenin-7-O-glucoside, and a saponin derivative (Soyasaponin I).

Quercetin (m/z 381.0, RT 1.45 min) was detected as one of the prominent flavonoids. Its molecular ion peak and characteristic fragment ions (m/z 151, 179) confirmed its presence. Quercetin is widely reported in medicinal plants and is known for potent antioxidant and anti-inflammatory effects, suggesting that it may contribute significantly to the bioactivity of the extract. Rutin (m/z 653.2, RT 2.10 min) was identified as a glycosylated flavonoid. Its fragmentation pattern, showing losses of sugar moieties, further validated this assignment. Rutin (quercetin-3-rutinoside) is commonly reported in plant extracts and is associated with vascular protective and radical-scavenging properties. Kaempferol-3-O-rutinoside (m/z 595.2, RT 3.87 min) was also detected. Its spectral data showed characteristic glycosidic fragment losses, confirming its identity. Kaempferol glycosides are often linked to anti-cancer and cardioprotective effects, highlighting the potential pharmacological relevance of this extract. Apigenin-7-O-glucoside (m/z 565.2, RT 5.51 min) was tentatively identified based on its protonated molecular ion and the typical neutral loss of glucose (162 Da). Apigenin derivatives are known for their anti-inflammatory and neuroprotective effects, indicating possible therapeutic

contributions from this compound. A high molecular weight compound (m/z 784.7, RT 8.86 min) was tentatively classified as a triterpenoid saponin derivative. The late elution profile and fragmentation involving sugar moieties are characteristic of saponins. Such compounds are often reported for their immunomodulatory, anticancer, and antimicrobial activities.

Overall, the LC-HRMS profiling demonstrated that the extract is rich in flavonoids and saponins, both of which are bioactive classes of natural products. The co-occurrence of quercetin, rutin, and glycosylated flavonoids indicates strong antioxidant potential, while the presence of saponins suggests additional pharmacological benefits. These findings provide a chemical basis for the traditional medicinal uses of the plant.

Table 1. Tentative Identification of Major Phytoconstituents

Peak ID	Retention Time (min)	Observed m/z	Tentative Compound	Justification
1	1.45	381.0	Quercetin	Matched m/z with known flavonoid; common in plant extracts
7	2.10	653.2	Rutin	Fragment pattern and m/z consistent with glycosylated flavonoid
11	3.87	595.2	Kaempferol-3-O-rutinoside	Consistent m/z and fragmentation with literature
20	5.51	565.2	Apigenin-7-O-glucoside	Molecular ion and RT match expected values
39	8.86	784.7	Saponin derivative (Soyasaponin I)	High m/z typical for saponin-type molecules

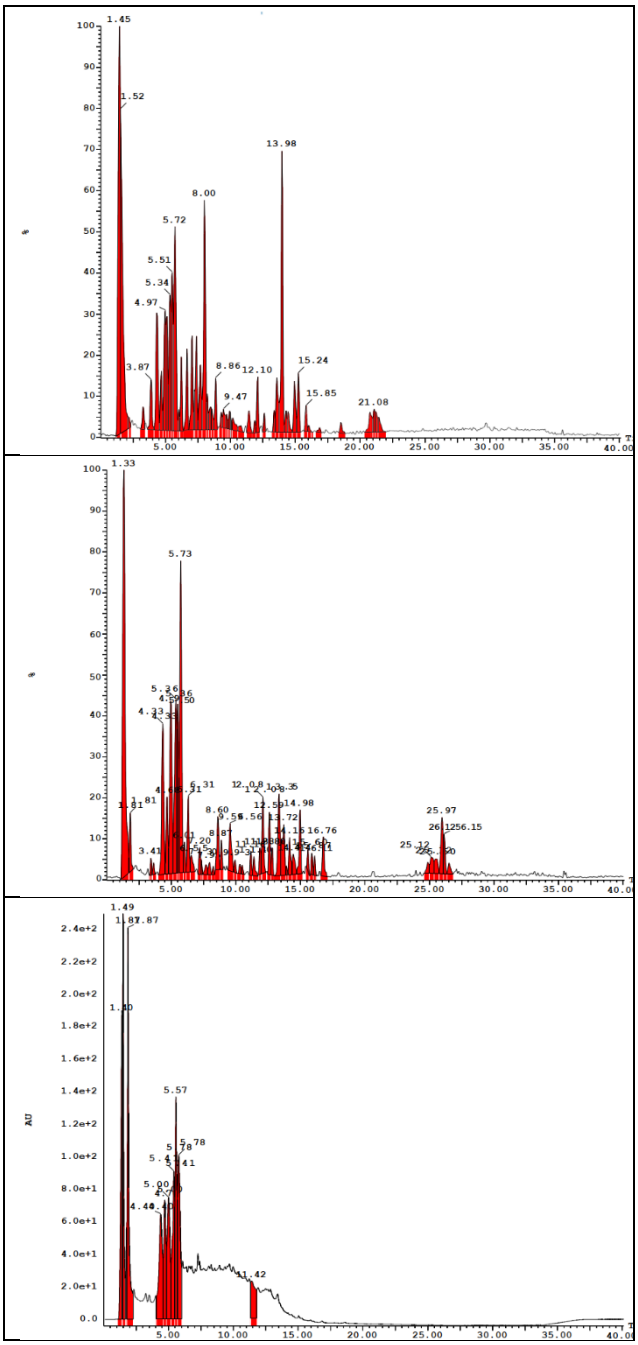

Figure 6. LC-HRMS graph of *B. monosperma* extract.

Molecular Docking

The molecular docking analysis of *B. monosperma* constituents targeting Insulin-like Growth Factor Receptor Type-2 (IGF2R) reveals interesting insights when compared to the NL-2V5O (Native Ligand) (Table 2). The NL-2V5O exhibits a docking score of -6.6 kcal/mol, forming conventional hydrogen bonds with VAL1793 and CYS1795, as well as electrostatic and hydrophobic interactions. Among the tested compounds, rutin demonstrates the highest binding affinity with a docking score of -9.3 kcal/mol, surpassing the NL-2V5O. Rutin forms multiple conventional hydrogen bonds with residues SER1659, ASP1662, ILE1660, ARG1768, LYS1851, and ARG1868, along with carbon hydrogen bonds, electrostatic interactions, and hydrophobic interactions. This extensive

network of interactions likely contributes to its superior binding affinity. Quercetin follows with a docking score of -8.2 kcal/mol, forming hydrogen bonds with ILE1660 and ASN1889, and engaging in various electrostatic and hydrophobic interactions. Apigenin-7-O-glucoside and kaempferol-3-rutinoside both exhibits docking scores of -7.6 kcal/mol, slightly better than the NL-2V5O. These compounds form hydrogen bonds with different residues and engage in electrostatic and hydrophobic interactions, suggesting diverse binding modes. Soyasaponin I show a docking score of -6.9 kcal/mol, comparable to the NL-2V5O, forming numerous hydrogen bonds with residues including VAL1793, CYS1795, and ASP1797. The analysis of bond types, lengths, and interacting residues provides valuable information on the binding mechanisms of these compounds. The superior binding affinities of rutin and quercetin, in particular, suggest their potential as lead compounds for further investigation in IGF2R-targeted drug development. Table 3 shows 2D and 3D interactions of selected derivatives and NL-2V5O with IGF2R.

Table 2. Binding interactions of selected compounds and NL-2V5O with IGF2R (PDBID: 2V5O)

Amino acid residues	Bond Length	Bond Type	Bond Category	Ligand Energy (Kcal/mol)	Docking Score
NL-2V5O					
VAL1793	2.64742	Hydrogen Bond	Conventional Hydrogen Bond	506.19	-6.6
CYS1795	2.21297				
CYS1795	2.2619				
ARG1868	2.43516				
ARG1868	2.92921				
ARG1868	3.33705	Electrostatic	Pi-Cation		
PRO1792	3.73838	Hydrophobic	Amide-Pi Stacked		
VAL1793	5.47454		Pi-Alkyl		
Apigenin-7-O-glucoside					
CYS1795	2.6753	Hydrogen Bond	Conventional Hydrogen Bond	994.14	-7.6
ASN1656	2.18052				
VAL1661	3.69727		Carbon Hydrogen Bond		
ARG1868	4.10827	Electrostatic	Pi-Cation		
ASP1797	4.81633				
ASP1797	2.6395	Hydrogen Bond	Pi-Donor Hydrogen Bond		
VAL1661	5.35546	Hydrophobic	Pi-Alkyl		
PRO1796	5.39625				
VAL1793	5.12989				
VAL1799	5.39823				
Kaempferol-3-rutinoside					
ASP1662	2.10235	Hydrogen Bond	Conventional Hydrogen Bond	1590.99	-7.6
VAL1793	2.35445				
ASN1656	2.3138				
ASN1656	2.67452				
ASP1797	4.50099	Electrostatic	Pi-Anion		
ASP1852	4.33922				
ASP1797	3.14084	Hydrogen Bond	Pi-Donor Hydrogen Bond		
VAL1661	4.42065	Hydrophobic	Pi-Alkyl		
PRO1796	5.3669				
Quercetin					
ILE1660	2.66184	Hydrogen Bond	Conventional Hydrogen Bond	181.05	-8.2
ASN1889	2.27444				
ARG1768	3.09538				
ARG1868	3.139	Electrostatic	Pi-Cation		

ARG1868	3.88668				
ARG1868	4.15641				
ASP1797	4.79363		Pi-Anion		
PRO1792	3.94685	Hydrophobic	Amide-Pi Stacked		
ARG1768	5.25894		Pi-Alkyl		
CYS1795	4.99073				
VAL1793	5.20079				
Rutin					
SER1659	2.9299	Hydrogen Bond	Conventional Hydrogen Bond	1639.89	-9.3
ASP1662	1.80594				
ILE1660	2.07447				
ARG1768	2.66781				
LYS1851	2.19363				
ARG1868	2.54886				
SER1659	3.48673		Carbon Hydrogen Bond		
SER1659	3.52984				
ARG1868	3.37691				
ARG1868	3.5687	Electrostatic	Pi-Cation		
ARG1868	3.62312				
ASP1852	4.05989		Pi-Anion		
ILE1660	3.83929	Hydrophobic	Pi-Sigma		
VAL1793	5.23648		Pi-Alkyl		
PRO1792	5.45488				
CYS1795	5.0315				
VAL1661	4.61439				
Soyasaponin I					
VAL1793	2.93572	Hydrogen Bond	Conventional Hydrogen Bond	945.03	-6.9
CYS1795	2.44308				
ILE1660	3.04587				
ASN1656	2.4542				
SER1659	2.74531				
ASN1656	2.42632				
ASN1656	2.32455				
SER1658	2.86106				
SER1659	2.92949				
ASP1797	2.23092				
VAL1794	3.55452		Carbon Hydrogen Bond		
SER1659	3.08673				
PRO1796	4.11519	Hydrophobic	Alkyl		
MET1801	4.52601				
PRO1796	5.45322				
VAL1799	4.85228				

Table 3. 2D and 3D interactions of selected derivatives with IGF2R.

2D Interactions	3D Interactions
NL-2V5O	
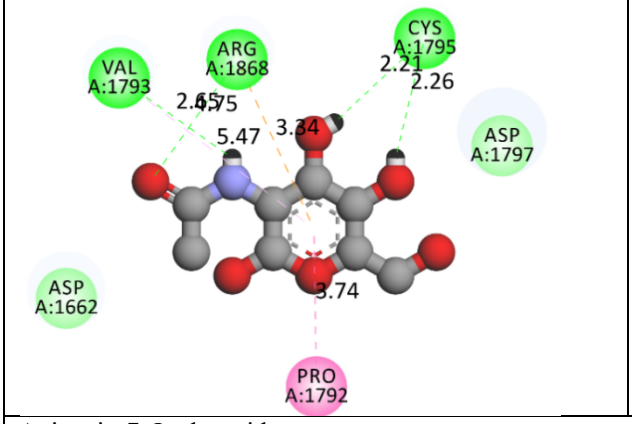	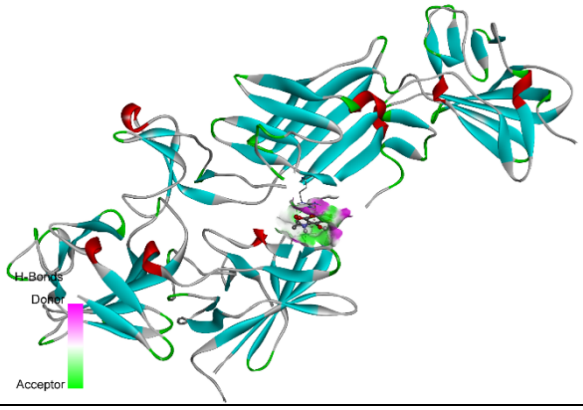
Apigenin-7-O-glucoside	
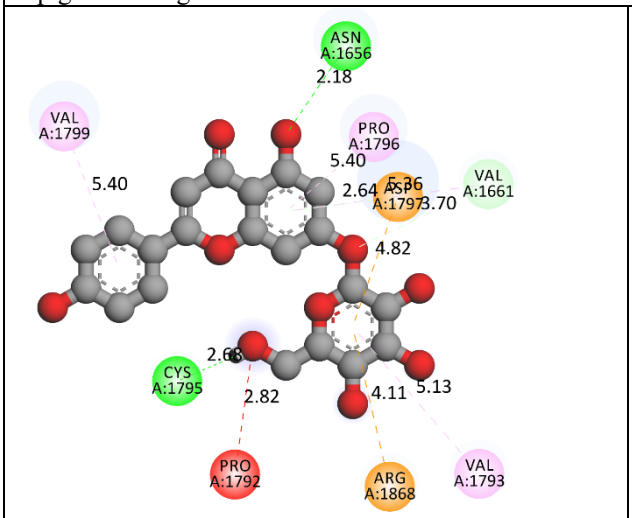	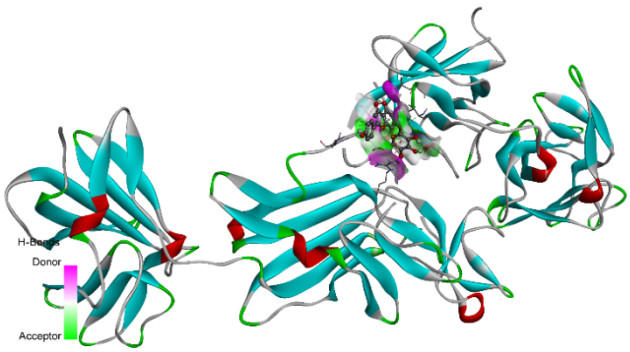
Kaempferol-3-rutinoside	
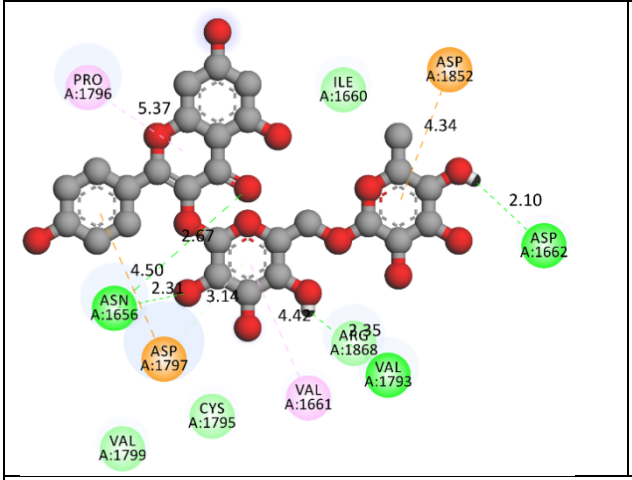	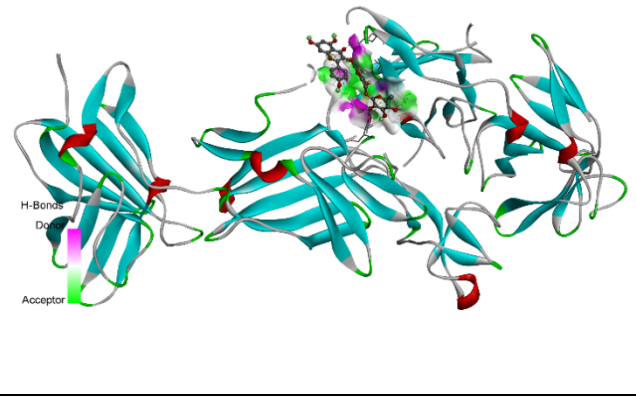
Quercetin	

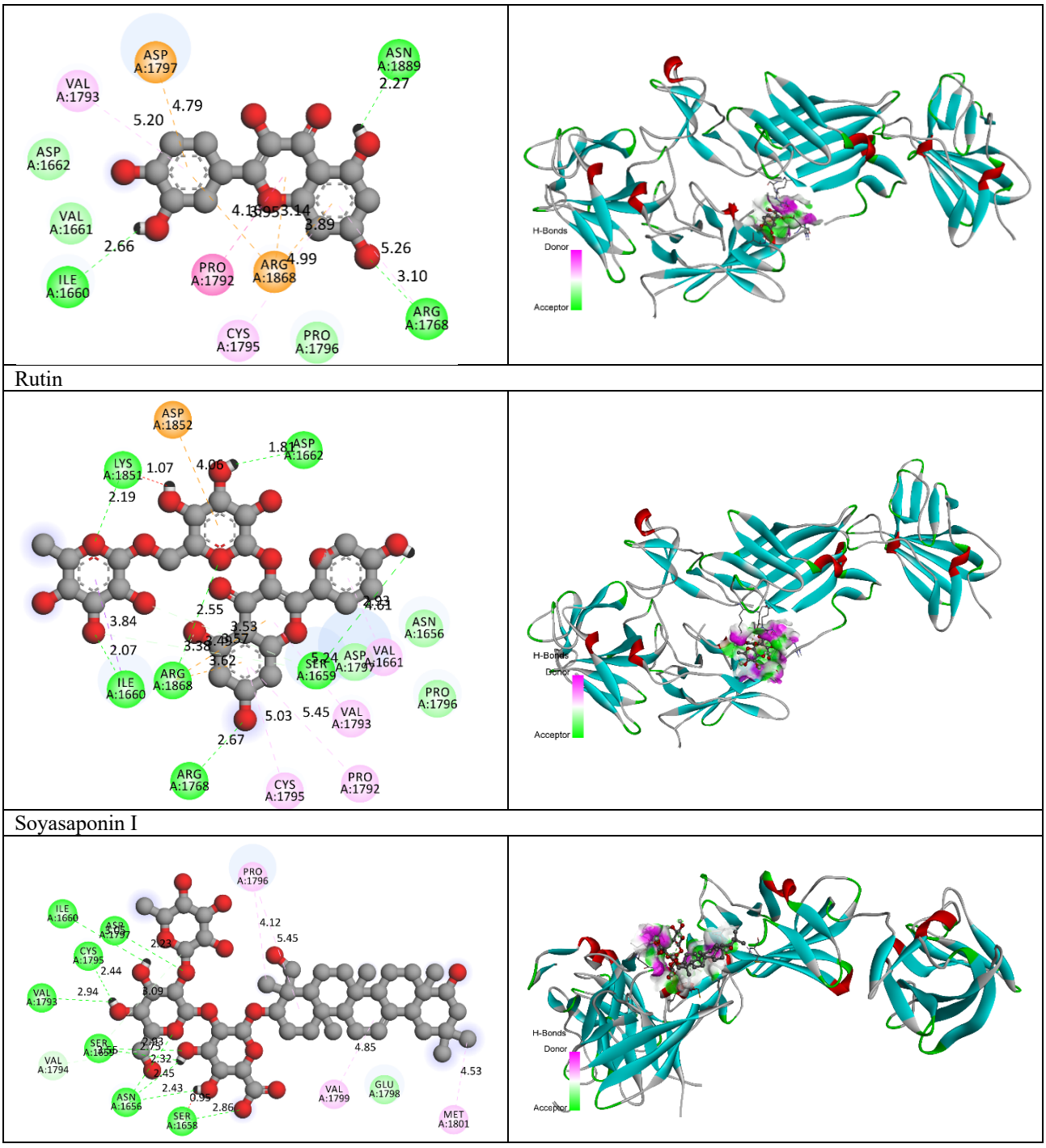

ADMET Analysis

Table 4 outlines the key physicochemical descriptors important for drug behavior. The NL-2V5O NL-2V5O exhibits the lowest molecular weight (MW: 221.09 g/mol), total polar surface area (TPSA: 119.25 Å²), and LogP (−1.80), suggesting high water solubility and moderate lipophilicity. Compared to this, all selected phytoconstituents from *B. monosperma* are significantly heavier and bulkier, particularly Soyasaponin I (MW: 928.5 g/mol), which may impact membrane permeability. Compounds like Apigenin-7-O-glucoside and Quercetin show a more favorable balance of TPSA and LogP (170.05 Å² and 1.08; 131.36 Å² and 1.44, respectively), indicating potential for oral bioavailability. However, compounds such as Rutin and Kaempferol-3-rutinoside, with TPSA above 200 Å², may suffer from poor intestinal absorption. Notably, all candidates except NL-2V5O and Quercetin have higher molecular complexity, which may negatively influence passive permeability.

Table 5 reveals that NL-2V5O adheres well to drug-likeness criteria, violating none of the major rules and showing a moderate QED score (0.337). Among the phytochemicals, Quercetin stands out with a higher QED (0.434), indicating greater drug-likeness. It also only violates the chelator rule,

which is relatively minor. In contrast, Rutin, Kaempferol-3-rutinoside, and Soyasaponin I violate multiple drug-likeness filters, especially the Lipinski rule, due to their large size and excessive hydrogen bond donors/acceptors. Their Golden Triangle and GSK rule violations suggest poor balance between potency and ADMET properties. Apigenin-7-O-glucoside, while showing moderate drug-likeness (QED: 0.331), may be considered promising due to its low violation profile.

According to Table 6, the NL-2V5O NL-2V5O shows excellent human intestinal absorption (HIA: 0.94) and bioavailability across all thresholds (F20%, F30%, F50%). In contrast, the flavonoid derivatives like Apigenin-7-O-glucoside, Kaempferol-3-rutinoside, and Rutin show drastically reduced HIA (<0.64), likely due to high TPSA and molecular size. Interestingly, Soyasaponin I, despite its size, maintains a high HIA (0.96) and excellent oral bioavailability, potentially due to interaction with transporters. Quercetin presents a good compromise between permeability and bioavailability, though its HIA (0.13) is unexpectedly low, indicating potential issues with absorption despite favorable drug-likeness.

Table 7 reveals a contrast in plasma protein binding (PPB) and blood-brain barrier (BBB) penetration. NL-2V5O has low PPB (13.95%) and moderate BBB permeability (0.44), supporting systemic and CNS activity. On the other hand, most phytochemicals have high PPB (>80%) and extremely low BBB values (<0.005), suggesting restricted CNS access, which may or may not be relevant depending on the therapeutic context. Quercetin again proves unique, with very high PPB (~99%) but minimal BBB permeability. In terms of metabolism, Quercetin shows extensive inhibition and substrate activity across multiple CYP450 isoforms, indicating a higher risk of drug–drug interactions. The other compounds generally show lower or negligible CYP interactions, with Rutin and Soyasaponin I displaying favorable metabolic profiles with minimal enzyme interference.

Excretion and toxicity profiles (Table 8) further differentiate the compounds. Quercetin demonstrates a notably high plasma clearance (CL: 8.28 mL/min/kg), suggesting rapid elimination, while Soyasaponin I shows extremely low clearance (0.0047), indicating potential accumulation. In terms of toxicity, NL-2V5O has moderate hepatotoxicity (H-HT: 0.55), while Quercetin and Soyasaponin I present contrasting profiles—Quercetin shows relatively lower hepatotoxicity but higher DILI risk. Rutin and Kaempferol-3-rutinoside demonstrate favorable safety, with low toxicity scores across most categories. Notably, Soyasaponin I presents higher hepatotoxicity and respiratory toxicity, raising safety concerns despite its bioavailability.

As shown in Table 9, all phytochemicals exhibit higher bio-concentration factor (BCF) and aquatic toxicity (IGC50, LC50FM, LC50DM) than the NL-2V5O, indicating potential for bioaccumulation and ecological impact. Quercetin and Soyasaponin I exhibit the highest aquatic toxicity values, which may limit their environmental suitability despite pharmacological promise. the NL-2V5O NL-2V5O maintains strong overall pharmacokinetic and safety profiles, select *B. monosperma* phytochemicals—particularly Quercetin and Apigenin-7-O-glucoside—show favorable drug-likeness, absorption potential, and moderate toxicity. However, their limited CNS permeability and potential metabolic interactions need consideration. Other derivatives like Rutin and Soyasaponin I offer strong bioavailability but may be restricted due to size, toxicity, or excretion limitations. Quercetin emerges as the most balanced lead, warranting further optimization and formulation strategies to address its bioavailability and interaction profile. ADMET radar of all selected compounds and NL2V5O are depicted in Table 10.

Table 4. Physicochemical properties of selected derivatives

Compounds	MW	Volume	Dense	nHA	nHD	nRot	nRing	TPSA	logS	logP
NL-2V5O	221.09	199.4695	1.10839	7	5	3	1	119.25	0.274001	-1.80564
Apigenin-7-O-glucoside	432.11	404.3569	1.068635	10	6	4	4	170.05	-3.4623	1.081711
Kaempferol-3-rutinoside	594.16	543.5275	1.093155	15	9	6	5	249.2	-2.55675	1.160389
Quercetin	302.04	282.7668	1.068159	7	5	1	3	131.36	-3.72159	1.447712
Rutin	610.15	552.3177	1.104708	16	10	6	5	269.43	-2.39666	0.986122
Soyasaponin I	928.5	905.9673	1.024871	18	11	9	8	294.98	-3.87352	1.677957

Table 5. Drug-likeness properties of designed derivatives

Compounds	QED	NP Score	Lipinski Rule	Pfizer Rule	GSK Rule	GoldenTriangle	Chelator Rule
NL-2V5O	0.337	2.019	0	0	0	0	0
Apigenin-7-O-glucoside	0.331	1.934	0	0	1	0	0
Kaempferol-3-rutinoside	0.159	1.945	1	0	1	1	0
Quercetin	0.434	1.701	0	0	0	0	1
Rutin	0.14	2.015	1	0	1	1	1
Soyasaponin I	0.11	2.312	1	0	1	1	0

Table 6. Absorption parameter of selected compounds

Compounds	Caco-2 Permeability	MDCK Permeability	Pgp-inhibitor	Pgp-substrate	HIA	F20%	F30%	F50%
NL-2V5O	-6.37263	-5.12885	0.002236	0.880931	0.94665	0.180412	0.97263	0.795713
Apigenin-7-O-glucoside	-6.39802	-5.00547	0.000156	0.310777	0.170933	0.214092	0.970167	0.991586
Kaempferol-3-rutinoside	-6.53241	-5.0288	5.12E-07	0.923982	0.136693	0.157615	0.989903	0.99919
Quercetin	-6.17681	-4.92272	0.027569	0.030731	0.133589	0.5038	0.99108	0.998593
Rutin	-6.54652	-5.02701	6.22E-08	0.699256	0.639735	0.772111	0.999751	0.999936
Soyasaponin I	-6.14022	-5.21764	4.56E-12	0.193695	0.961041	0.898941	0.994859	0.999958

Table 7. Distribution and metabolism parameter of selected molecules

Compounds	Distribution				Metabolism									
					CYP1A2		CYP2C19		CYP2C9		CYP2D6		CYP3A4	
	PPB%	VD	BBB	Fu	Inhibitor	Substrate	Inhibitor	Substrate	Inhibitor	Substrate	Inhibitor	Substrate	Inhibitor	Substrate
NL-2V5O	13.95247	-0.52554	0.438822	88.68793	0.004324	0.000106	0.001866	3.30E-05	0.235022	0.0008688	0.01661	0.001371	0.000138	0.000132
Apigenin-7-O-glucoside	81.81997	-0.04141	0.003269	16.72626	0.0366	4.91E-05	1.04E-05	5.75E-07	8.04E-05	0.0016042	0.000577	0.000894	0.13445	3.97E-06
Kaempferol-3-rutinoside	85.11787	-0.03781	8.18E-05	13.38901	3.72E-05	0.006566	2.55E-06	1.59E-06	9.67E-06	0.0000247	2.16E-05	4.18E-06	0.027368	1.93E-07
Quercetin	98.65997	-0.87913	0.000445	1.131221	0.998312	0.38429	0.005855	4.87E-05	0.432249	0.0029644	0.00018	0.978297	0.936699	1.34E-06
Rutin	85.0054	-0.0	3.59E-05	14.65911	0.001	0.00364	1.44E-07	1.07E-06	1.85E-06	7.47E-05	2.26E-06	1.48E-07	0.029205	2.29E-09

		5883												
Soyasaponin I	67.48967	-0.46428	0.004134	21.59202	5.04E-17	5.27E-09	2.60E-13	0.000714	8.49E-09	8.03E-05	1.65E-09	4.06E-07	3.73E-07	2.24E-05

Table 8. Excretion and Toxicity parameters of selected compounds

Compounds	Excretion		Toxicity										
	CL-plasma	T1/2	H-HT	DILI	Ames Toxicity	Rat Oral Acute Toxicity	FDA MDD	Skin Sensitization	Carcinogenicity	Eye Corrosion	Eye Irritation	Respiratory Toxicity	
NL-2V5O	1.772639	2.328189	0.55989	0.495928	0.796281	0.046798	0.018939	0.957543	0.173344	0.000456	0.752 77	0.060898	
Apigenin-7-O-glucoside	3.044592	3.564608	0.535201	0.935421	0.852867	0.072883	0.216398	0.945562	0.556581	3.97E-05	0.736176	0.083734	
Kaempferol-3-rutinoside	1.414836	4.271624	0.462769	0.914587	0.73364	0.045293	0.148402	0.983965	0.079052	3.09E-05	0.894723	0.034867	
Quercetin	8.288988	1.585 75	0.337382	0.782596	0.586042	0.479917	0.788757	0.896924	0.600177	0.603284	0.998417	0.673657	
Rutin	1.610724	4.616005	0.406325	0.936922	0.756376	0.044139	0.137174	0.997444	0.046632	3.59E-05	0.904546	0.030272	
Soyasaponin I	0.004726	3.645359	0.712121	0.877409	0.381924	0.007973	0.034616	0.999879	0.154816	8.17E-09	0.000753	0.009876	

Table 9. Environmental toxicity profile of designed molecules

Compounds	BCF	IGC50	LC50FM	LC50DM
NL-2V5O	0.091368	1.715961	2.298723	2.971279
Apigenin-7-O-glucoside	0.48361	2.996276	3.604573	4.334037
Kaempferol-3-rutinoside	0.561833	3.177655	3.798183	4.488873
Quercetin	1.210035	3.758566	4.112	4.485008
Rutin	0.533413	3.180953	3.927314	4.680011
Soyasaponin I	0.894253	3.546674	4.140287	5.157055

Table 10. ADMET radar of selected derivatives and NL-2V5O

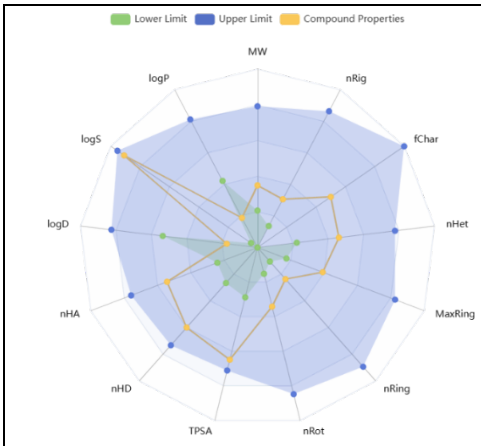 NL-2V5O	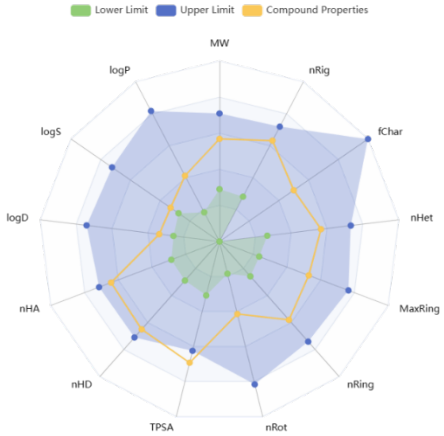 Apigenin-7-O-glucoside
 Kaempferol-3-rutinoside	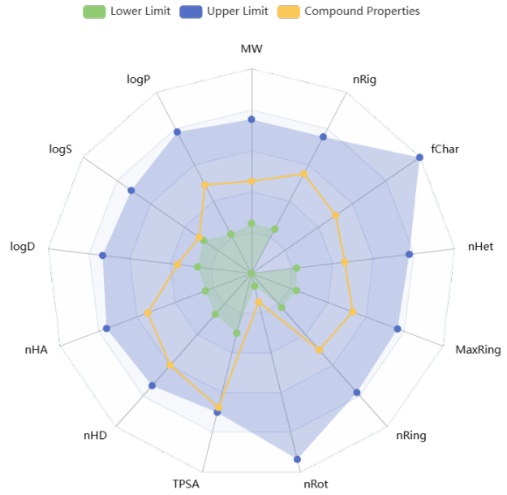 Quercetin
 Rutin	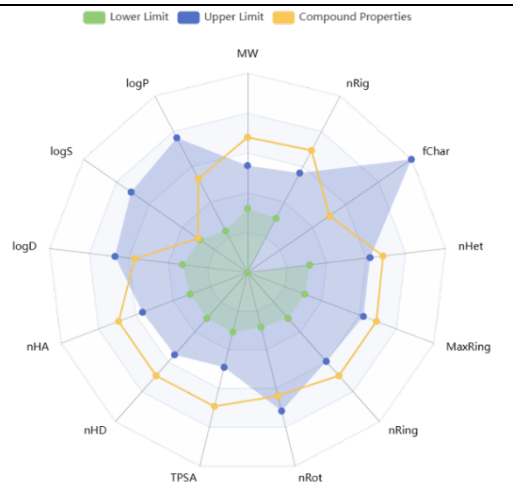 Soyasaponin I

CONCLUSION

The present investigation comprehensively evaluated the hydroalcoholic extract of *B. monosperma* through organoleptic, physicochemical, microbial, phytochemical, LC-HRMS, molecular docking, and ADMET analyses. Organoleptic and physicochemical characterization confirmed that the extract is pure, stable, and safe, with low moisture content, acceptable ash values, absence of

contaminants, and no detectable heavy metals or pesticide residues. The near-neutral pH and favorable extractive values indicated suitability for oral and topical applications, while the higher alcohol-soluble fraction suggested enrichment of flavonoids and triterpenoids. Microbial testing further validated its safety, confirming freedom from pathogenic organisms. Preliminary phytochemical screening revealed abundant phenolics and flavonoids, along with glycosidic compounds, saponins, and tannins, supporting its potential for antioxidant, cardioprotective, and immunomodulatory activities. LC-HRMS analysis provided deeper insight into the chemical profile, tentatively identifying bioactive constituents such as quercetin, rutin, kaempferol-3-O-rutinoside, apigenin-7-O-glucoside, and soyasaponin I. These compounds are widely recognized for their pharmacological benefits, including antioxidant, anti-inflammatory, neuroprotective, and anticancer effects, thereby offering a phytochemical basis for the traditional therapeutic use of *B. monosperma*. Molecular docking studies targeting IGF2R highlighted rutin and quercetin as top-performing ligands with stronger binding affinities than the NL-2V5O, indicating their potential as lead molecules in drug development. ADMET predictions revealed that quercetin, despite some absorption challenges and high protein binding, displayed the most balanced drug-likeness profile, whereas other compounds showed limitations due to size, permeability, or toxicity. Collectively, the findings validate the therapeutic promise of *B. monosperma*, particularly its flavonoid-rich composition, as a source of antioxidant and pharmacologically active molecules. Among the identified phytochemicals, quercetin emerges as the most promising lead candidate, meriting further in vivo evaluation, formulation strategies to enhance bioavailability, and safety assessments to support its potential development into effective herbal or modern therapeutic agents.

.

REFERENCES

1. Chaughule RS, Barve RS. Role of herbal medicines in the treatment of infectious diseases. Vegetos. 2024;37(1):41–51.
2. Jahromi B, Pirvulescu I, Candido KD, Knezevic NN. Herbal medicine for pain management: Efficacy and drug interactions. Pharmaceutics. 2021;13(2):1–43.
3. Plotnikoff GA, Lillehei AS. Herbal medicines. Complement Ther Nurs Promot Integr Care. 2022; p. 378–93.
4. Stathakis T, Economou L, Barda M, Angelioudakis T, Kati V, Karamaouna F. Potential of hedgerows with aromatic plants as reservoirs of natural enemies of pests in orange orchards. Insects. 2023;14(4).
5. Blay-Roger R, Bach W, Bobadilla LF, Reina TR, Odriozola JA, Amils R, et al. Natural hydrogen in the energy transition: Fundamentals, promise, and enigmas. Renew Sustain Energy Rev. 2024;189.
6. Tandon R, Shivanna KR, Mohan Ram HY. Reproductive biology of B. monosperma (Fabaceae). Ann Bot. 2003;92(5):715–23.
7. Rai A, Pandey VC, Singh AK, Ghoshal N, Singh N. B. monosperma: A leguminous species for sustainable forestry programmes. Environ Dev Sustain. 2021;23(6):8492–505.
8. Sindhia V, Bairwa R. Plant review: B. monosperma. Int J Pharm Clin Res. 2010;2(2).
9. Pattanayak S, Mollick MMR, Maity D, Chakraborty S, Dash SK, Chattopadhyay S, et al. B. monosperma bark extract mediated green synthesis of silver nanoparticles: Characterization and biomedical applications. J Saudi Chem Soc. 2017;21(6):673–84.
10. Aryal B, Adhikari B, Aryal N, Bhattarai BR, Khadayat K, Parajuli N. LC-HRMS profiling and antidiabetic, antioxidant, and antibacterial activities of Acacia catechu (L.f.) Willd. Biomed Res Int. 2021;2021.
11. Windarsih A, Bakar NKA, Dachriyanus, Yuliana ND, Riswanto FDO, Rohman A. Analysis of pork in beef sausages using LC-Orbitrap HRMS untargeted metabolomics combined with chemometrics for halal authentication study. Molecules. 2023;28(16).
12. Heinsvig PJ, Noble C, Dalsgaard PW, Mardal M. Forensic drug screening by liquid chromatography hyphenated with high-resolution mass spectrometry (LC-HRMS). TrAC Trends Anal Chem. 2023;162.
13. Tamboli AS, Tayade SD. In-depth investigation of berberine and tropane through computational screening as possible DPP-IV inhibitors for the treatment of T2DM. J Pharm Sci Comput Chem. 2025;1(1):1–11.
14. Siddiqui FA, Makhloufi R, Hojjati M, El-sayed MS, Eman K. Computational exploration of quinine and mefloquine as potential anti-malarial agents. J Pharm Sci Comput Chem. 2025;1(2):106–15.
15. Ahmed SA, Tabassum PS, Falak SA, Vikhar A, Ahmad D, Shaikh S. Molecular docking and network pharmacology: Investigating Vitis vinifera phytoconstituents as multi-target therapeutic agents against breast cancer. J Pharm Sci Comput Chem. 2025;1(2):116–34.
16. Jadhav SS, Dighe PR, Kumbhare MR. Synthesis, in vitro evaluation, and molecular docking studies of novel pyrazoline derivatives as promising bioactive molecules. J Pharm Sci Comput Chem. 2025;1(3).
17. Chen C, Zhang Y, Zhang Y, Li J, Tsao SW, Zhang MY. Superior antitumor activity of a novel bispecific antibody co-targeting human epidermal growth factor receptor 2 and type I insulin-like growth factor receptor. Mol Cancer Ther. 2013;13(1):90–100.
18. Barlow DP, Stöger R, Herrmann BG, Saito K, Schweifer N. The mouse insulin-like growth factor type-2 receptor is imprinted and closely linked to the Tme locus. Nature. 1991;349(6304):84–7.

19. Ekyalongo RC, Yee D. Revisiting the IGF-1R as a breast cancer target. npj Precis Oncol. 2017;1(1).
20. El-Shewy HM, Lee MH, Obeid LM, Jaffa AA, Luttrell LM. The IGF-1 and IGF-2/mannose-6-phosphate receptors independently regulate ERK1/2 activity in HEK293 cells. J Biol Chem 2007;282(36):26150–7.
21. Sharma V, Janmeda P. Extraction, isolation and identification of flavonoid from Euphorbia neriifolia leaves. Arab J Chem. 2017;10(4):509–14.
22. Nickavar B, Mojab F, Javidnia K, Roodgar Amoli MA. Chemical composition of the fixed and volatile oils of Nigella sativa L. from Iran. Z Naturforsch C J Biosci. 2003;58(9–10):629–31.
23. Talreja T, Kumar M, Goswami A, Gahlot G, Jinger A, Sharma T. HPLC analysis of saponins in Achyranthes aspera and Cissus quadrangularis. Pharma Innov J. 2017;6(1):76–9.
24. Khandelwal KR. Practical Pharmacognosy: Techniques and Experiments. 20th ed. Pune: Nirali Prakashan; 2005. p. 150–3.
25. Mukherjee PK. Quality Control of Herbal Drugs: An Approach to Evaluation of Botanicals. New Delhi: Business Horizons; 2002. 800 p.
26. Singh M, Tamboli ET, Kamal YT, Ahmad W, Ansari SH, Ahmad S. Quality control and in vitro antioxidant potential of Coriandrum sativum Linn. J Pharm Bioallied Sci. 2015;7:280–3.
27. Kamal Y, Singh M, Salam S, Ahmad S. Standardization of Unani polyherbal formulation Qurse-e-Hummaz: A comprehensive approach.Drug Dev Ther. 2016;7(1):39.
28. Chaudhari RN, Khan SL, Chaudhary RS, Jain SP, Siddiqui FA. β-Sitosterol: Isolation from Muntingia calabura Linn bark extract, structural elucidation and molecular docking studies as potential inhibitor of SARS-CoV-2 Mpro (COVID-19). Asian J Pharm Clin Res. 2020;13(5):204–9.
29. Indrayanto G. Recent development of quality control methods for herbal-derived drug preparations. Nat Prod Commun. 2018;13(12):1599–606.
30. Al-Busaid MM, Akhtar MS, Alam T, Aly Shehata W. Development and evaluation of herbal cream containing curcumin from Curcuma longa. Pharm Pharmacol Int J. 2020;8(5):285–9.
31. Vasincu A, Luca SV, Charalambous C, Neophytou CM, Skalicka-Woźniak K, Miron A. LC-HRMS/MS phytochemical profiling of Vernonia kotschyana: Potential involvement of highly oxygenated stigmastane-type saponins in cancer cell viability and apoptosis. S Afr J Bot. 2022;144:83–91.
32. Luca SV, Minceva M, Gertsch J, Skalicka-Woźniak K. LC-HRMS/MS-based phytochemical profiling of Piper spices: Association of piperamides with endocannabinoid system modulation. Food Res Int. 2021;141.
33. Kızıltaş H, Bingöl Z, Gören AC, Pinar SM, Alwasel SH, Gülçin İ. LC-HRMS profiling of phytochemicals and antidiabetic, anticholinergic and antioxidant activities of Astragalus brachycaly extract. J Chem Metrol. 2021;15(2):135–51
.